STEM CELLS AND DEVELOPMENT
Volume 23, Number 15, 2014

DOI: 10.1089/scd.2013.0628

Generation of V2a Interneurons from Mouse Embryonic Stem Cells

Chelsea R. Brown,* Jessica C. Butts,* Dylan A. McCreedy, and Shelly E. Sakiyama-Elbert

V2a interneurons of the ventral spinal cord and hindbrain play an important role in the central pattern generators (CPGs) involved in locomotion, skilled reaching, and respiration. However, sources of V2a interneurons for in vitro studies are limited. In this study, we developed a differentiation protocol for V2a interneurons from mouse embryonic stem cells (mESCs). Cells were induced in a $2^{-}/4^{+}$ induction protocol with varying concentrations of retinoic acid (RA) and the mild sonic hedgehog (Shh) agonist purmorphamine (Pur) in order to increase the expression of V2a interneuron transcription factors (eg, Chx10). Notch signaling, which influences the commitment of p2 progenitor cells to V2a or V2b interneurons, was inhibited in cell cultures to increase the percentage of V2a interneurons. At the end of the induction period, cell commitment was assessed using quantitative real-time polymerase chain reaction, immunocytochemistry, and flow cytometry to quantify expression of transcription factors specific to V2a interneurons and the adjacent ventral spinal cord regions. Low concentrations of RA and high concentrations of Pur led to greater expression of transcription factors specific for V2a interneurons. Notch inhibition favored V2a interneuron over V2b interneuron differentiation. The protocol established in this study can be used to further elucidate the pathways involved in V2a interneuron differentiation and help produce sources of V2a interneurons for developmental neurobiology, electrophysiology, and transplantation studies.

Introduction

Pluripotent embryonic stem cells (ESCs) hold the potential to differentiate into any cell type within the body, including neurons and glia of the central nervous system (CNS). This differentiation depends upon the complex interaction of signaling molecules, the extent of which are just beginning to be understood in CNS development. ESCs provide a useful tool to study pathways involved in differentiation and neurological disorders, and to characterize properties of CNS neurons. They can also be used to generate sources of neurons for cell-replacement therapies following injury to the CNS. Differentiation protocols have been established to obtain a variety of neural cell types from ESCs, including motoneurons [1,2], dopaminergic neurons [3–5], cortical neurons [6], cerebellar neurons [7], retinal rods and cones [8], and peripheral neurons [9]. Protocols to obtain other spinal neurons from ESCs still need to be established.

V2a interneurons are actively involved in the central pattern generators (CPGs) and propriospinal networks [10] of the spinal cord and the respiratory centers of the hindbrain. Recent research has shown that V2a interneurons in the ventral spinal cord run ipsilaterally, display rhythmicity, and provide excitatory input to CPG interneurons and propriospinal networks [10–12]. Genetic ablation of V2a in mice leads to the loss of left-right coordination during locomotor activities [11], whereas targeted ablation of cervical V2a subpopulations leads to deficits in reaching movements [10]. Cells homologous to V2a interneurons in zebrafish have been shown to span greater than two spinal cord segments and synapse onto motoneurons [13]. Recently, V2a interneurons in the medial reticular formation of the hindbrain have been shown to stimulate excitatory signals to produce regular breathing patterns. Mice with genetic ablation of V2a interneurons display irregular and less frequent breathing patterns, leading to decreased survival rates of newborns [14].

During the development of the ventral spinal cord, differentiation depends upon the interplay of retinoic acid (RA) released from the somites [15] and the ventral-dorsal gradient of sonic hedgehog (Shh) released from the floor plate and notochord [16–18]. RA, an inducer of neural differentiation, has been shown to affect the rostral-caudal identity of cells in vitro with higher concentrations inducing a more caudal cell type [15]. This signaling along with the Shh gradient gives rise to four ventral progenitor interneuron domains (p0–p3) and a progenitor motor neuron domain (pMN) arranged along the ventral-dorsal axis as shown in

Department of Biomedical Engineering, Washington University in St. Louis, St. Louis, Missouri.
*These two authors contributed equally to this work.

Fig. 1 [16–22]. These progenitor domains mature to form four ventral interneuron classes (V0–V3) and motoneurons [20,21].

Distinct combinations of homeodomain (HD) and basic-helix-loop-helix (bHLH) transcription factors, controlled by the precise patterning of RA and Shh expression, can identify both the progenitor domains and the mature neuronal populations, as shown in Fig. 1. Cells in the p2 progenitor domain express Irx3, Lhx3, and Foxn4 [19–21,23–25] and mature into three distinct interneuron classes, V2a, V2b, and V2c. V2a interneurons are excitatory, glutamatergic, and express Chx10 and Lhx3 [17,18,26], whereas V2b interneurons are inhibitory, GABAergic/glycinergic, and express Gata3 [24,27–32]. Newly identified V2c interneurons arise from a subset of V2b interneurons, and their function in CPG networks is still unknown [33,34]. Endogenous Notch-1 signaling has been shown to influence the fate of p2 progenitors, with high Notch-1 signaling favoring differentiation into V2b interneurons over V2a interneurons [25].

Several recent studies have examined the electrophysiological properties of V2a interneurons in vivo. The lack of in vitro sources of V2a interneurons, however, may limit future studies. While some neural cell types can be obtained from primary mouse spinal cord tissue, obtaining substantial interneuron cell populations, such as V2a interneurons, remains difficult [35]. In this study, we developed a novel protocol to provide a source of V2a interneurons from ESCs both for developmental neurobiology studies and potential cell-based therapies. Existing protocols for motoneuron differentiation from mouse ESCs (mESCs) use RA and Shh signaling to drive differentiation of cells with a cervical spinal identity [2,36]. Since V2a interneuron pools lay more rostral in respiratory columns in the medial reticular formation of the hindbrain [14], we hypothesize that a lower RA concentration could promote differentiation of ESCs into V2a interneurons. We explored the effect of RA concentration on the expression of p2 progenitor and V2a markers. Hox markers, transcription factors expressed along the rostral-caudal axis of the spinal cord, were also evaluated. The effect of varying the level of Shh signaling on the expression of transcription factors expressed in p2 progenitors and V2a interneurons was also determined. Since Chx10 is also expressed in photoreceptor progenitor cells, the absence of another photoreceptor progenitor marker (Crx) was used to confirm the spinal fate of the induced cells [37,38]. Inhibition of the Notch-1 signaling was also evaluated to determine the effect of Notch signaling on the number of $Chx10^+$ V2a interneurons and $Gata3^+$ V2b interneurons. In conclusion, we have identified a protocol for the differentiation of V2a interneurons from mESCs.

Materials and Methods

ESC culture

RW4 mESCs derived from Sv129 mice (gift from Dr. David Gottlieb, Washington University) were used for all induction experiments. mESCs were cultured in complete media consisting of Dulbecco's modified Eagle's medium (DMEM; Invitrogen, Carlsbad, CA) supplemented with 10% newborn calf serum (Invitrogen), 10% fetal bovine serum (Invitrogen), 1× nucleosides (Embryomax, Millipore, Billenca, MA), 1,000 U/mL leukemia inhibitory factor (LIF; Millipore), and 100 μM beta-mercaptoethanol (BME; Invitrogen). Cells were passaged every 2 days at a 1:5 ratio and seeded onto a T-25 flask coated overnight with a 0.1% gelatin solution (Sigma, St. Louis, MO).

Differentiation of mESCs

mESCs were differentiated using a $2^-/4^+$ induction protocol [1,2]. One million mESCs were suspended in DKF5

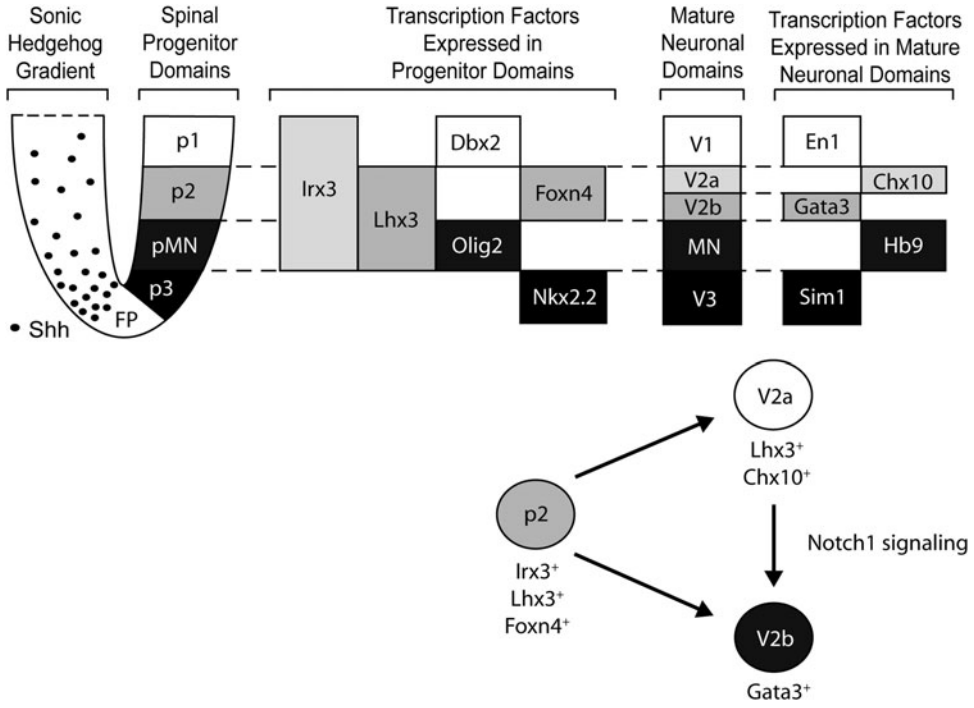

FIG. 1. Schematic showing the transcription factors expressed in the ventral half of the developing neural tube. The ventral-to-dorsal gradient of sonic hedgehog (Shh) and relative positions of progenitor domains are shown on the *left*. The transcription factors expressed by both interneuron (p1–p3) and motoneuron (pMN) progenitor domains are shown in the *middle*. The progenitor domains mature into committed interneuron (V0–V3) and motoneuron (MN) cell types that express a different set of transcription factors, shown on the *far right*. Cells in the p2 progenitor domain differentiate into both V2a and V2b interneurons, with Notch-1 signaling favoring V2b subtypes over V2a subtypes. FP, floor plate.

media consisting of DMEM/F12 (Invitrogen) supplemented with 5% knockout replacement serum, 1× insulin transferrin-selenium (Invitrogen), 1× nonessential amino acids (Invitrogen), 1× nucleosides (Emrbyomax, Millipore), and 100 μM β-mercaptoethanol (Invitrogen) in a 100-mm-diameter dish coated with 0.1% agar solution (Fisher Scientific, Waltham, MA). Cells were cultured in suspension for 2 days (2^-) to form embryoid bodies (EBs).

EBs were plated onto dishes coated with a 0.1% gelatin solution with the addition of DFK5 media: 0.01–2 μM RA (Sigma) and 0.1–1.5 μM Pur (Calbiochem EMD, Billencia, MA) or 0.6 μM smoothened agonist (SAG; Calbiochem EMD), with a media change every 2 days. Transcription factor expression was assessed at the end of the $2^-/4^+$ induction.

Following the $2^-/4^+$ induction, cells were dissociated using 0.25% trypsin EDTA and incubated at 37°C for 20 min. The cells were then quenched with 3× complete media and centrifuged at 240 *g* for 5 min. Cells were re-suspended in DFK5 media with purmorphamine (Pur), RA, and 5 μM *N*-[*N*-(3,5-difluorophenacetyl-L-alanyl)]-(*S*)-phenylglycine t-butyl ester (DAPT; Sigma) and placed on a laminin-coated plate for 4 h.

Laminin-coated plates

Tissue-culture-treated six-well plates were coated with a 0.005% polyornithine solution (Sigma) at 37°C for 1 h. The plate was then washed five times with sterile phosphate-buffered saline (PBS) and coated overnight with a 5 μg/mL laminin solution (Invitrogen) at 4°C. The laminin solution was then removed and the plate was washed once with sterile PBS before cell seeding.

Immunocytochemistry

Following the $2^-/4^+$ induction, cell cultures were fixed with 4% paraformaldehyde (Sigma) for 30 min and permeabilized with a 0.01% Triton X-100 (Sigma) solution for 15 min. Cells were blocked with 5% normal goat serum (NGS; Sigma) in PBS for 1 h at 4°C. Primary antibodies were added to PBS with 2% NGS and incubated at 4°C overnight. Primary antibodies were added at the following ratios: mouse anti-Chx10 (1:1,000; Santa Cruz, Santa Cruz, CA), mouse anti-Hb9 (1:20; Developmental Studies Hybridoma Bank [DSHB], Iowa City, IA), mouse anti-Lhx3 (1:1,000, Lim3; DSHB), and rabbit anti-B-tub III (1:1,000; Covance, Princeton, NJ). Following primary antibody incubation, three 15-min washes with PBS were applied. Appropriate Alexa Fluor secondary antibodies (1:200; Invitrogen) in PBS with 2% NGS were filtered with a 0.22-μm filter and added to the cultures overnight at 4°C. Three 15-min washes with PBS were applied. Cell nuclei were stained with the nuclei marker Hoechst (1:1,000; Invitrogen) or DAPI (0.5 μg/mL; Sigma). Cultures were imaged with a 20× objective on an Olympus IX70 inverted microscope. Images were processed using Abobe Photoshop CS2 (Adobe, San Jose, CA).

Quantitative real-time polymerase chain reaction analysis

The RNA from EBs was extracted using RNeasy Mini Kit (Qiagen, Valencia, CA) following the $2^-/4^+$ induction. cDNA was synthesized from RNA using High Capacity RNA-to-cDNA Kit (Invitrogen). The cDNA was combined with TaqMan Gene Expression Assays (Applied Biosystems, Carlsbad, CA; Supplementary Table S1; Supplementary Data are available online at www.liebertpub.com/scd) and TaqMan Fast Advanced Master Mix (Applied Biosystems) and quantitative real-time polymerase chain reaction (qRT-PCR) was performed using a Step One Plus Applied Biosystems thermocyler with the following protocol: 95°C for 20 s; 40 cycles of 95°C for 1 s and 60°C for 20 s. The number of cycles necessary for the fluorescent intensity to increase exponentially, known as the threshold cycle (C_t), was recorded as the relative mRNA expression. To account for differences in mRNA amounts, target genes were normalized to β-actin expression. The comparative ΔC_t method [39] was used to analyze the mRNA expression levels in cultures induced with 10 nM RA and 10 nM, 100 nM, 250 nM, 500 nM, or 1 μM Pur compared with control cultures induced with 0 nM Pur and 10 nM RA; cultures induced with 1 μM Pur and 10 nM, 50 nM, 100 nM, 2 μM, or 10 μM RA compared with control cultures induced with 1 μM Pur and 0 nM RA; and cultures induced with 1 μM Pur, 10 nM RA, and 5 μM DAPT added on day 4 of induction compared with control cultures induced with 1 μM Pur, 10 nM RA, and 0 μM DAPT. Fold differences in relative mRNA expression levels over the control cultures are reported for each gene ($n = 3$ for all groups).

Statistical analysis

For qRT-PCR and flow cytometry experiments, three replicates of each condition were analyzed. Statistical analysis using Statistica software (version 5.5) was performed. Significance was determined using Scheffe's *post hoc* test for analysis of variance (ANOVA) with 95% confidence. Average values are reported with error bars indicating the standard error of the mean (SEM).

Flow cytometry

Immediately following the induction protocol, EBs were stained for flow cytometry. Cultures were dissociated with 0.25% trypsin-EDTA (Invitrogen) for 20 min. Excess volume of complete media was added to quench the trypsin, and cultures were triturated to form single-cell suspensions. Cells were centrifuged at 230 *g* for 5 min, the media was removed, and the cells were fixed with 2% paraformaldehyde (Sigma). For permeabilization and staining, the Transcription Factor Buffer Set (BD Pharmingen 562725, Franklin Lakes, NJ) was used according to manufacturer's instructions with mouse anti-Chx10 (1:1,000) primary antibodies and appropriate Alexa Fluor secondary antibodies (1:200; Invitrogen). Following the protocol, nuclei were stained with DAPI (0.5 μg/mL; Sigma) for 5 min. For each culture, 10,000 events were recorded using a Canto II flow cytometer (Becton Dickinson, Franklin Lakes, NJ). Data analysis was performed using FloJo software (FloJo, Ashland, OR). Debris was removed using the forward scatter versus side scatter and DAPI fluorescence versus forward scatter plots. Control groups of cells stained with only secondary antibodies were used to determine gating parameters. Results of the flow cytometry are presented as percentage of $Chx10^+$ cells out of the total $DAPI^+$ population.

Results

Effect of Pur concentration on gene expression

To analyze the effects of increasing Shh signaling (using the Shh agonist Pur) on neural gene expression, qRT-PCR and antibody staining were performed. mESCs were induced with 10 nM RA and 10 nM–1 μM of Pur using a $2^-/4^+$ induction protocol. Relative gene expression was analyzed using qRT-PCR by comparing mRNA expression levels of the induction groups to a control culture induced with 0 nM Pur and 10 nM RA ($n = 3$ for each condition). Expression for Chx10, Hb9, and Lhx3 at 1 μM Pur (and 10 nM RA) showed a significant increase over all other Pur groups shown in Fig. 2a. Similarly, Foxn4 and Gata3 mRNA expression at 1 μM Pur showed a significant increase over 10 nM Pur, 100 nM Pur, and 250 nM Pur groups.

To determine whether further increasing Shh signaling increases Chx10 expression, cell cultures were induced in a $2^-/4^+$ induction with 10 nM RA and either 1 μM Pur, 1.5 μM Pur, or 0.6 μM smoothened agonist (SAG), a stronger Shh agonist than Pur. At the end of the induction, mRNA expression levels were measured using qRT-PCR. Increasing Shh signaling with 1.5 μM Pur or 0.6 μM SAG resulted in downregulation of Chx10 expression (Fig. 2b), indicating that 1 μM of the milder agonist Pur is best for increasing yield of $Chx10^+$ cells. Hb9 expression decreased at 1.5 μM Pur compared with 1 μM Pur. However, Hb9 expression was upregulated twofold at 0.6 μM SAG compared to 1 μM Pur, which is expected because a higher amount of Shh signaling is present in the more ventral MN domain. This data also suggests possible toxic effects at 1.5 μM Pur.

Immunocytochemistry confirmed that Chx10 protein levels mirrored the results from qRT-PCR. mESCs were induced with the same conditions as stated earlier. Chx10 staining at the end of the $2^-/4^+$ protocol appeared to increase with increasing Pur concentration. The 1 μM Pur group displayed the highest amount of Chx10 staining, as shown in Fig. 2c–n.

Expression of Crx, the photoreceptor progenitor marker, was examined to ensure that retinal cell types were not being induced. Expression of Crx at the mRNA levels (Fig. 2o) decreased compared with the control cultures induced with 0 nM Pur and 10 nM RA, and did not change significantly with increasing Pur concentrations, indicating a retinal cell type was in fact not being induced.

Effect of RA concentration on gene expression

To analyze the effects of RA concentration on neural and V2a interneuron gene expression, qRT-PCR and immunocytochemistry staining were performed. mESCs were induced with 1 μM Pur and 10 nM–10 μM RA using a $2^-/4^+$ protocol, as shown in the schematic in Fig. 3a. Relative gene expression was analyzed using qRT-PCR by comparing mRNA expression levels in each induction group to control cultures induced with 1 μM Pur and 0 nM RA ($n = 3$ for each condition). When RA concentration was increased from 10 nM to 10 μM, Chx10 expression decreased approximately fourfold (Fig. 3b). Chx10 mRNA expression levels in the 10 nM RA and 50 nM RA groups were similar and both showed a significant increase over the 2 μM RA and 10 μM RA groups, indicating that lower concentrations of RA are better for differentiation of $Chx10^+$ cells. Similar results were observed with mRNA expression levels of the V2b marker Gata3 (Fig. 3b). Irx3 mRNA expression levels in the 10 nM RA group show a significant increase over all other groups. No significant differences were found in the expression levels of the p2 progenitor transcription factor Foxn4. Increasing RA concentration did not lead to significant changes in the mRNA expression levels of Lhx3 and Hb9—transcription factors for the pMN and p2 progenitor domains and the motoneuron domain, respectively (Fig. 3c). To confirm Chx10 expression in induced cultures, antibody staining was performed following the $2^-/4^+$ induction protocol. Greater Chx10 staining was observed in cultures receiving 10 nM RA and 100 nM RA, and less Chx10 staining was seen when the RA concentration was increased to 2 μM (Fig. 3d), again supporting that lower RA concentrations relative to standard MN differentiation protocols give a higher yield of $Chx10^+$ cells.

Effect of RA concentration on positional and retinal gene expression

RA has been shown to influence rostral-caudal positional identity in the spinal cord. To determine the effect of RA concentration on the rostral-caudal identity, Hox gene expression was analyzed using qRT-PCR at the end of the $2^-/4^+$ induction protocol. Expression of the more caudal spinal marker Hoxc8 increased with increasing RA concentration (Fig. 4a). Expression of Hoxc5, a more rostral spinal marker, and Hox3a, a hindbrain marker, did not change with increasing RA. Overall, the expression of H3a showed lower fold changes over the control (0 nM RA) than either Hoxc5 or Hoxc8 (Fig. 4b).

Chx10 expression has also been observed in developing retinal progenitor cells. To determine whether lower RA concentration induced differentiation into retinal progenitors, the expression of Crx was investigated using qRT-PCR. Downregulation of Crx expression in the presence of RA was observed compared with controls receiving 1 μM Pur and 0 nM RA. No significant changes in Crx mRNA expression levels were found when RA was increased from 10 nM to 10 μM (Fig. 4c). These results indicate that a retinal cell type is not being induced using this differentiation protocol.

Effect of Notch signaling on Chx10 expression

To analyze the effects of Notch signaling inhibition on Chx10 expression, DAPT, a Notch-1 inhibitor, was added on day 4 of the $2^-/4^+$ induction as shown in the schematic in Fig. 5a. At the end of the $2^-/4^+$ induction, relative mRNA expression levels were compared with control cultures induced with 1 μM Pur, 10 nM RA, and 0 μM DAPT ($n = 3$ for each condition) by qRT-PCR. Chx10 mRNA was upregulated and Gata3 mRNA was downregulated with the addition of DAPT (Fig. 5b), indicating Notch inhibition increases V2a commitment over V2b. To quantify the $Chx10^+$ cell populations, flow cytometry was performed on mESCs induced with or without DAPT. At the end of the induction, cell cultures were labeled with Chx10 antibodies and DAPI, and flow cytometry was performed ($n = 3$ for each condition).

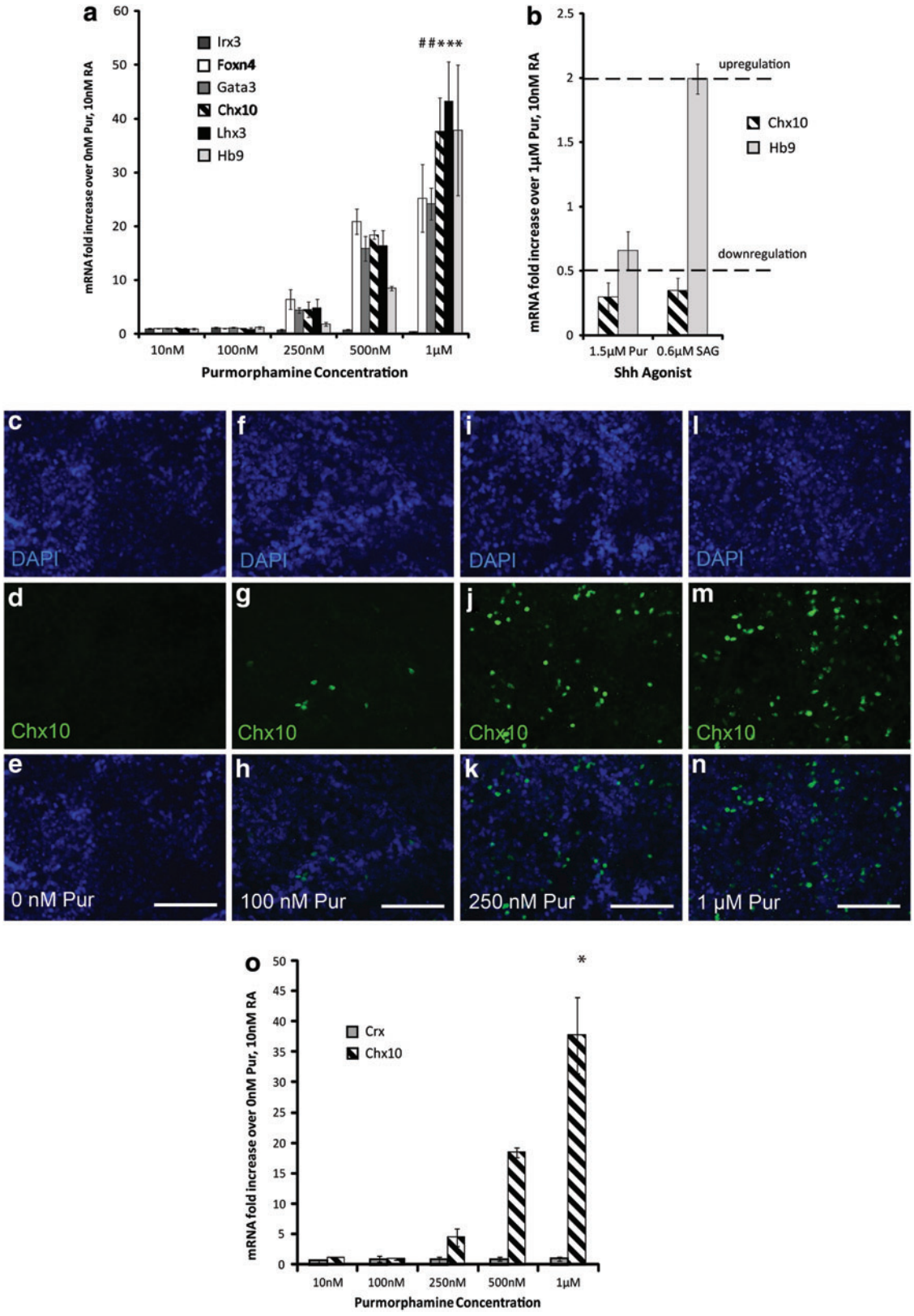

FIG. 2. Effect of Pur concentration on neural gene expression. **(a–b)** Quantitative real-time polymerase chain reaction (qRT-PCR) results ($n=3$) at the end of the $2^{-}/4^{+}$ induction showing mRNA levels for progenitor and mature transcription factors compared with control cultures induced with 0 nM purmorphamine (Pur) and 10 nM retinoic acid (RA). *Dotted lines* denote upregulation and downregulation. Embryoid bodies (EBs) induced with 10 nM RA and 0 nM Pur **(c–e)**, 100 nM Pur **(f–h)**, 250 nM **(i–k)**, and 1 μM **(l–n)** stained with DAPI, Chx10 antibodies, and overlayed. **(o)** qRT-PCR results ($n=3$) at the end of the $2^{-}/4^{+}$ induction showing mRNA expression levels for the photoreceptor progenitor transcription factor Crx compared with control cultures induced with 0 nM Pur and 10 nM RA. The symbol * denotes significance over 10, 100, 250, and 500 nM groups ($P<0.05$), the symbol # denotes significance over 10, 100, and 250 nM groups ($P<0.05$). Error bars denote SEM. Analysis was performed using Scheffe's post hoc test ($n=3$). Scale bars are 100 μm. Color images available online at www.liebertpub.com/scd

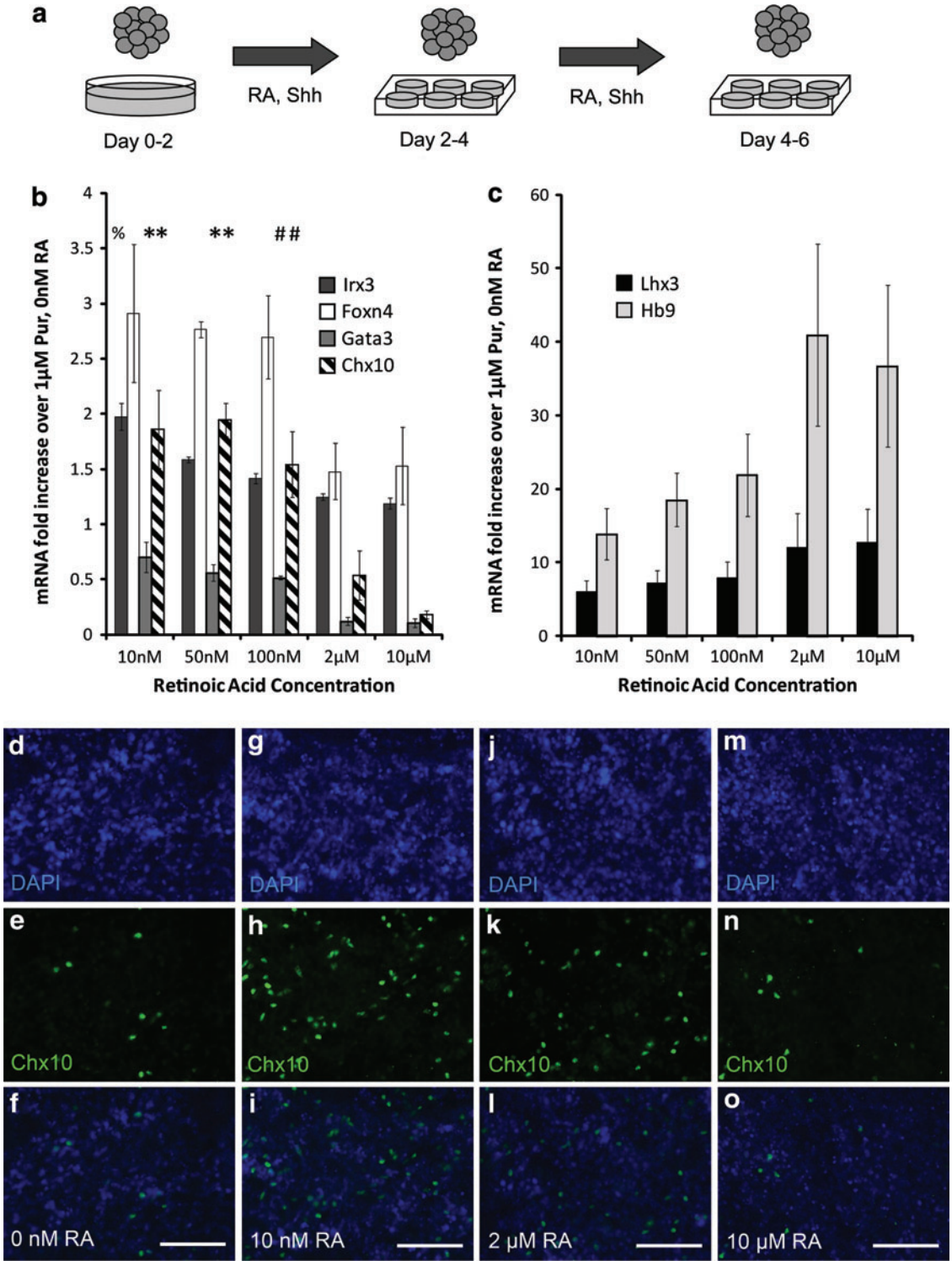

FIG. 3. Effect of RA concentration on gene expression. **(a)** Schematic showing the $2^{-}/4^{+}$ induction protocol of mESCs. **(b–c)** qRT-PCR results ($n=3$) at the end of the $2^{-}/4^{+}$ induction showing mRNA levels for progenitor and mature neural transcription factors compared with control cultures induced with 1 μM Pur and 0 nM RA. The symbol * denotes significance over 10 and 2 μM groups ($P<0.05$). The symbol # denotes significance over 10 μM group ($P<0.05$). The symbol % denotes significance over all other groups ($P<0.05$). Error bars denote SEM. Analysis was performed using Scheffe's post hoc test ($n=3$). EBs induced with 1 μM Pur and 0 nM RA **(d–f)**, 10 nM RA **(g–i)**, 2 μM **(j–l)**, and 10 μM **(m–o)** stained with DAPI, Chx10 antibodies, and overlayed. Scale bars are 100 μm. Color images available online at www.liebertpub.com/scd

In the absence of DAPT, 2.25% ± 0.94% of cells expressed Chx10, whereas 16.83% ± 2.11% of cells expressed Chx10 with the addition of DAPT, approximately an eightfold increase (Fig. 5c). Histograms of one trial for each group are shown in Fig. 5d and e. Immunocytochemistry performed on induced cultures confirmed the effects of DAPT (Fig. 5f).

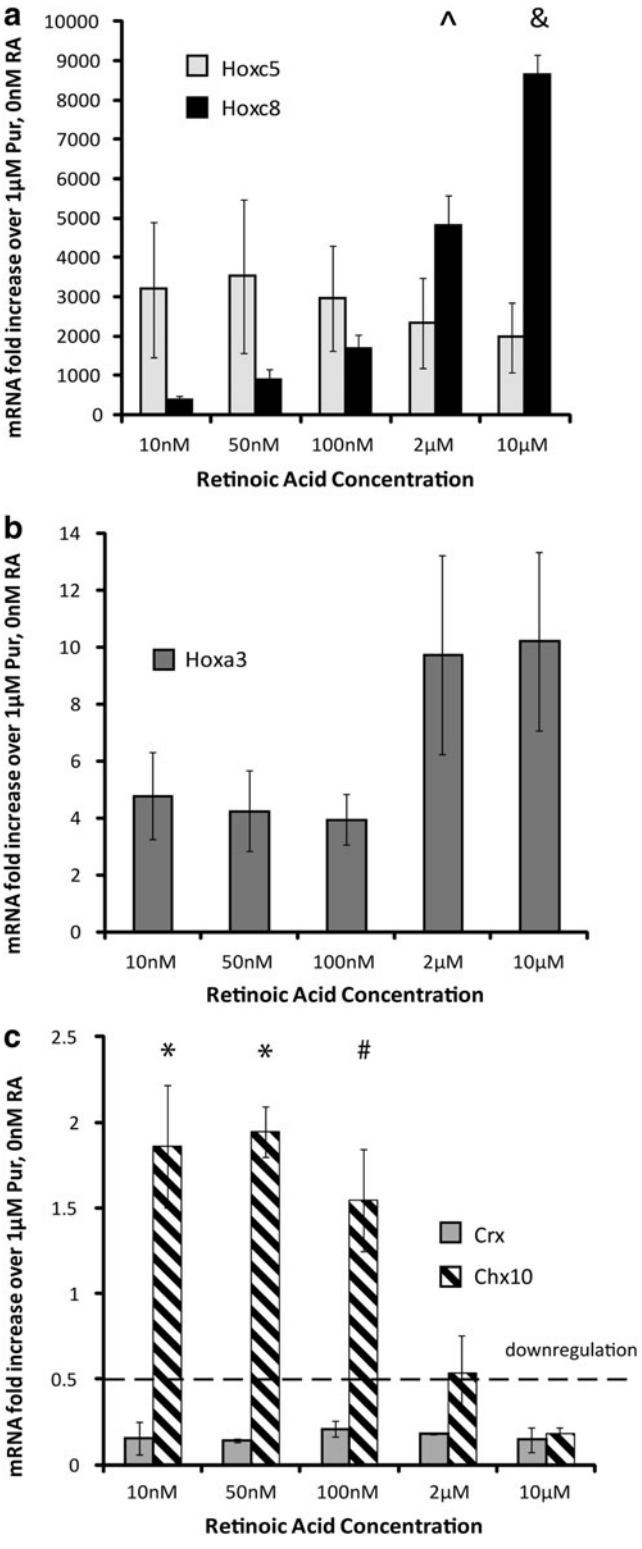

Neuronal marker expression in Chx10$^+$ cells

Immunocytochemistry was used to confirm the neuronal identity of Chx10$^+$ cells following the $2^-/4^+$ induction with 1 μM Pur, 10 nM RA, and 5 μM DAPT. Following the induction, cultures were dissociated and plated on laminin-coated plates for 4 h. Cultures were stained with DAPI and Chx10, Lhx3, or Hb9, and β-tubulin III (β-tub) antibodies. The majority of Chx10$^+$, Lhx3$^+$, and Hb9$^+$ cells stained positively for β-tub and displayed neurite projections as shown in Fig. 6.

Discussion

V2a interneurons have been shown to be involved in repetitive motor behaviors in the CPGs of the spinal cord and medial reticular formations of the hindbrain and play an important role in left-right coordination of locomotion, skilled reaching movements, and rhythmic patterning of breathing [10,14,26]. Differentiation of V2a interneurons from mESCs has the potential to increase understanding developmental pathways and possibly provide a source for cell therapies in high cervical spinal cord injuries affecting respiratory and motor function. While protocols for motoneurons from mESCs have been developed, a protocol to derive V2a interneurons has not yet been established [1,2]. In this study, we looked at the effects of a mild Shh agonist, Pur, and RA on neural differentiation to develop a protocol for generating V2a interneurons from mESCs.

Dorsoventral patterning of neuronal progenitor domains is controlled by Shh and RA signaling through activation of class I and class II HD and bHLH transcription factors 1 [16–22]. Using the protocol for differentiation of motoneurons from mESCs first developed by Wichterle et al. as a reference point, Shh and RA signaling levels were varied to find conditions that promoted V2a interneuron differentiation [1]. Development of V2a interneurons in the ventral neural tube is dependent on many factors, a major one being Shh signaling [40,41]. Increasing concentration of the mild Shh agonist Pur up to 1 μM increased Chx10 expression. Similar results were observed with other ventral neural tube markers—Hb9, Irx3, Gata3, Foxn4, and Lhx3. Higher Pur concentrations decreased both Chx10 and Hb9 expression possibly due to toxic effects. Greater Shh signaling, achieved by using a stronger Shh agonist, SAG, decreased

FIG. 4. Positional and retinal identity of induced cells. **(a–b)** qRT-PCR results ($n = 3$) at the end of the $2^-/4^+$ induction showing mRNA levels for positional Hox genes compared with control cultures induced with 1 μM Pur and 0 nM RA. **(c)** qRT-PCR results ($n = 3$) at the end of the $2^-/4^+$ induction showing mRNA levels for the photoreceptor progenitor transcription factor Crx compared with control cultures induced with 1 μM Pur and 0 nM RA. *Dotted line* denotes downregulation. The symbol & denotes significance over 10 nM, 50 nM, 100 nM, and 2 μM groups ($P < 0.05$). The symbol ^ denotes significance over 10, 50, and 100 nM ($P < 0.05$). The symbol * denotes significance over 10 and 2 μM groups ($P < 0.05$). The symbol # denotes significance over 10 μM group ($P < 0.05$). Error bars denote SEM. Analysis was performed using Scheffe's post hoc test ($n = 3$).

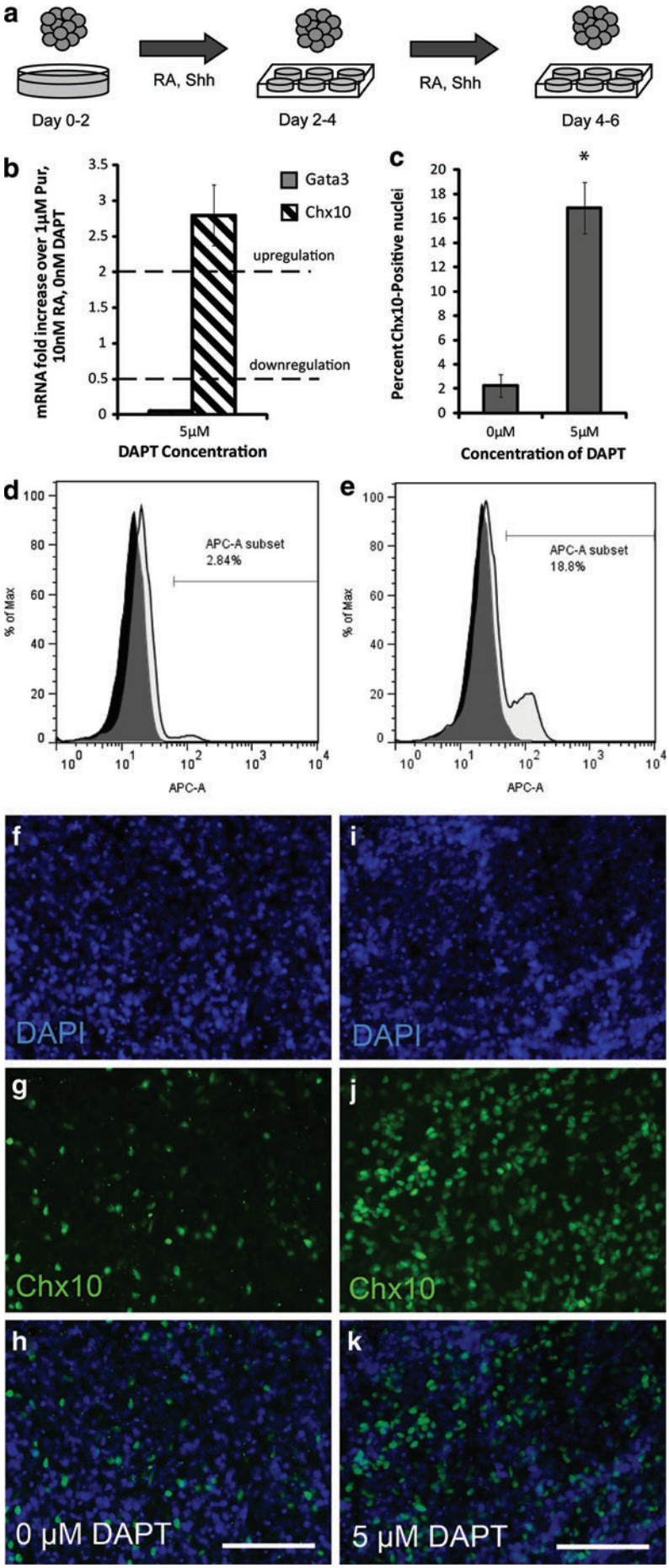

FIG. 5. Effect of DAPT on V2 interneuron subtype. **(a)** Schematic showing $2^-/4^+$ induction of mESCs with the addition of the Notch signaling inhibitor DAPT. **(b)** qRT-PCR results ($n=3$) at the end of the $2^-/4^+$ induction showing mRNA levels for progenitor and mature neural transcription factors compared with control cultures induced with 1 μM Pur and 10 nM RA. *Dotted lines* denote upregulation and downregulation. **(c)** Flow cytometry results ($n=3$) taken at the end of the $2^-/4^+$ induction protocol. **(d–e)** Histograms of flow cytometry results of one group induced without DAPT **(d)** and one group induced with DAPT **(e)**. **(f–h)** EBs induced with 1 μM Pur, 10 nM RA, and 0 μM DAPT stained with DAPI, Chx10 antibodies, and overlayed. **(i–k)** EBs induced with 1 μM Pur, 10 nM RA, and 5 μM DAPT stained with DAPI, Chx10 antibodies, and overlayed. The symbol * denotes significance over 0 nM DAPT ($P<0.05$). Error bars denote SEM. Analysis was performed using Scheffe's post hoc test ($n=3$). Scale bars are 100 μm. Color images available online at www.liebertpub.com/scd

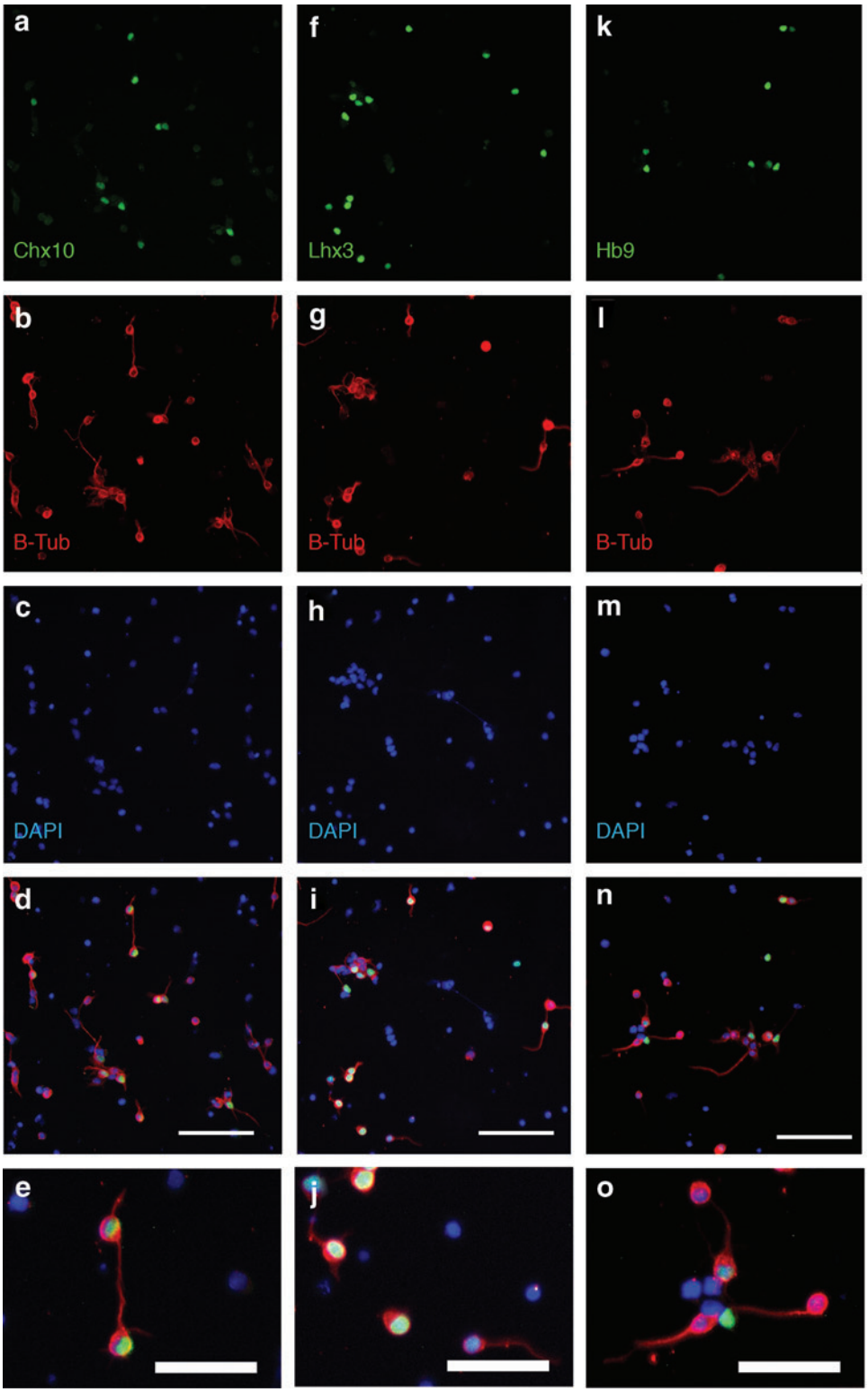

FIG. 6. Staining of dissociated cultures. Cultures induced with the $2^{-}/4^{+}$ protocol with 1 μM Pur, 10 nM RA, and 5 μM DAPT. Cultures were dissociated and stained with antibodies for Chx10, Lhx3, Hb9, and β-tubulin III (B-Tub), a neuronal marker. **(a–c)** Chx10 costained with B-Tub and DAPI. **(f–h)** Lhx3 costained with B-Tub and DAPI. **(k–m)** Hb9 costained with B-Tub and DAPI. The above images were overlayed **(d, i, n)** and enlarged to show neurite extension **(e, j, o)**. Scale bars are 100 μm. Color images available online at www.liebertpub.com/scd

Chx10 while increasing Hb9 expression [1,36,42]. We observed that a lower amount of Shh signaling is needed for Chx10 expression compared with Hb9, consistent with the ventral-to-dorsal Shh gradient found in the developing neural tube [40].

RA released from the somites during neural tube development is an inducer of neural differentiation and influences the rostral-caudal identity of cells in vitro with lower concentrations inducing more rostral cell types [15,43]. Studies have also shown that RA activates the expression of bHLH transcription factors to control the differentiation of neuronal cell types, such as V2a interneurons [44]. We hypothesized that by decreasing RA concentration we could promote the differentiation of V2a interneurons found

rostrally in respiratory columns of the medial reticular formation of the hindbrain [14]. Our experiments showed that decreasing RA concentration increased Chx10 expression. Similar results were seen with Gata3, a V2b interneuron marker, and the progenitor marker Irx3. However, RA concentration did not significantly affect the expression of the motoneuron marker Hb9. Chx10 expression was the greatest and did not change significantly between the 10 and 100 nM RA groups, suggesting that lower concentrations of RA increase V2a interneuron differentiation.

Addition of RA into the culture media has been shown to induce a cervical cell type [36]. Our experiments showed decreased expression of the brachial and thoracic spinal marker Hoxc8 at lower RA concentrations. This gives evidence that a more rostral cell type is being induced with lower concentrations of RA. The expression of Hoxc5, a cervical spinal marker, did not change with increasing RA concentration, indicating that our cultures retain spinal cord identity, even at low RA concentrations. The hindbrain/spinal marker Hoxa3 does not change with increasing RA concentration. There is a large population of Chx10-positive cells found in the respiratory column in the hindbrain, just rostral to the cervical spinal cord. Some of these cells may be present in our cultures; however, further testing would be needed to confirm the respiratory column cell identity.

The Chx10 transcription factor is also present in photoreceptor progenitor cells [38]. The protocol to differentiate this cell type uses low concentrations of RA [45]. Crx, a transcription factor present in photoreceptor progenitor development, does not change with increasing RA or Pur concentration and is downregulated compared with controls not receiving RA or Pur. These results indicate that decreasing the RA concentration to 10 nM does not induce a retinal cell type. Protocols to induce the retinal cell type from mESCs use basic fibroblast growth factor (bFGF) signaling in addition to low concentration of RA signaling [45]. Because we do not use bFGF signaling, it is possible that the addition of Shh signaling into the induction protocol keeps the cells of a spinal fate.

Notch signaling is involved in numerous pathways of development, and previous literature has shown Notch-1 signaling favors the commitment of p2 progenitors into the V2b interneurons over V2a interneurons [25]. Expression of Gata3, a V2b interneuron marker, was significantly downregulated while Chx10 expression was upregulated after addition of 5 μM DAPT to the induction media. Flow cytometry showed that addition of DAPT increased $Chx10^+$ cells almost eightfold. These results confirm that inhibition of Notch-1 signaling increases V2a commitment over V2b. Notch-1 signaling is also responsible for the proliferation of glial cell types [46]. It is possible that in addition to decreasing V2b commitment, the addition of DAPT is decreasing the glial population and increasing neuronal commitment.

To ensure whether the $Chx10^+$ cells being induced were neurons, staining with the neuronal marker β-tub was performed on cultures that were dissociated and plated the cells at a low density at the end of the induction. All Chx10-positive cells were colabeled with β-tub and displayed neurite extension. We performed preliminary studies to look at the maturation capabilities of the cells following the induction protocol. However, Chx10 is not a mature V2a interneuron marker, and we found that Chx10 expression diminished around 4 days of maturation. Also, we saw positive Vglut staining, a marker for vesicles involved in glutamate transport in mature neurons, beginning on day 4 and persisting through day 7 of culture (data not shown). While we cannot make a claim that our $Chx10^+$ cells are $Vglut^+$, we can conclude that our induction protocol does not prevent maturation of glutamatergic neurons. Future studies using more mature V2a interneuron markers, which have yet to be identified, could confirm the glutamatergic identity of the induced cells. Alternatively, the use of genetically modified mouse ESCs with lineage-tracing capability for *Chx10* may provide a reasonable substitute for these markers, but establishing these cell lines is beyond the scope of this study.

While protocols to differentiate motoneurons and other cell types from mESCs exist, protocols for the differentiation of ventral interneurons have yet to be established. We show that successful differentiation of $Chx10^+$ cells can be achieved using a mild Shh agonist, Pur, and a low RA concentration. The addition of a Notch signaling inhibitor increases Chx10 expression by favoring V2a differentiation over V2b. This protocol presents an opportunity to further the developmental understanding of V2a interneurons by providing an in vitro source of the cell type that currently does not exist. Further, this protocol has potential to be translated to human ESCs (hESCs). Protocols developed for induction of MNs from hESCs [47,48] show similarities to the previously established mESC protocols [1,42], and it is possible that similar steps can be taken to translate this protocol for V2a interneurons to hESCs. The type of signaling molecules and the concentrations used for MN differentiation from mESCs and hESCs are comparable, with the main difference being a longer time scale for hESC differentiation. Better understanding of this cell type can lead to advances in developmental neurobiology and can be applied to future differentiation protocols as well as transplantation therapies.

Acknowledgments

The authors were funded by the NIH RO1 grant 5R01NS051454. We would like to acknowledge Jonathan Yang for assistance with the preliminary maturation studies. We would also like to acknowledge the Hope Center for Neurological Disorders at Washington University in St. Louis, MO.

Author Disclosure Statement

No competing financial interests exist.

References

1. Wichterle H, I Lieberam, JA Porter and TM Jessell. (2002). Directed differentiation of embryonic stem cells into motor neurons. Cell 110:385–397.
2. Mccreedy DA, CR Rieger, DI Gottlieb and SE Sakiyama-Elbert. (2011). Transgenic enrichment of mouse embryonic stem cell-derived progenitor motor neurons. Stem Cell Res 8:368–378.
3. Lee SK and SL Pfaff. (2001). Transcriptional networks regulating neuronal identity in the developing spinal cord. Nat Neurosci 4 (Suppl):1183–1191.

4. Perrier AL, V Tabar, T Barberi, ME Rubio, J Bruses, N Topf, NL Harrison and L Studer. (2004). Derivation of midbrain dopamine neurons from human embryonic stem cells. Proc Natl Acad Sci U S A 101:12543–12548.
5. Yang D, Z-J Zhang, M Oldenburg, M Ayala and S-C Zhang. (2008). Human embryonic stem cell-derived dopaminergic neurons reverse functional deficit in parkinsonian rats. Stem Cells 26:55–63.
6. Gaspard N, T Bouschet, A Herpoel, G Naeije, J Van Den Ameele and P Vanderhaeghen. (2009). Generation of cortical neurons from mouse embryonic stem cells. Nat Protoc 4:1454–1463.
7. Salero E and ME Hatten. (2007). Differentiation of ES cells into cerebellar neurons. Proc Natl Acad Sci U S A 104: 2997–3002.
8. Osakada F, H Ikeda, M Mandai, T Wataya, K Watanabe, N Yoshimura, A Akaike, Y Sasai and M Takahashi. (2008). Toward the generation of rod and cone photoreceptors from mouse, monkey and human embryonic stem cells. Nat Biotechnol 26:215–224.
9. Lee G, H Kim, Y Elkabetz, G Al Shamy, G Panagiotakos, T Barberi, V Tabar and L Studer. (2007). Isolation and directed differentiation of neural crest stem cells derived from human embryonic stem cells. Nat Biotechnol 25: 1468–1475.
10. Azim E, J Jiang, B Alstermark and TM Jessell. (2014). Skilled reaching relies on a V2a propriospinal internal copy circuit. Nature [Epub ahead of print]; DOI: 10.1038/nature13021.
11. Crone SA, KA Quinlan, L Zagoraiou, S Droho, CE Restrepo, L Lundfald, T Endo, J Setlak, TM Jessell, O Kiehn and K Sharma. (2008). Genetic ablation of V2a ipsilateral interneurons disrupts left-right locomotor coordination in mammalian spinal cord. Neuron 60:70–83.
12. Dougherty KJ and O Kiehn. (2010). Firing and cellular properties of V2a interneurons in the rodent spinal cord. J Neurosci 30:24–37.
13. Eklöf-Ljunggren E, S Haupt, J Ausborn, I Dehnisch, P Uhlén, S-I Higashijima and A El Manira. (2012). Origin of excitation underlying locomotion in the spinal circuit of zebrafish. Proc Natl Acad Sci U S A 109:5511–5516.
14. Crone SA, JC Viemari, S Droho, A Mrejeru, JM Ramirez and K Sharma. (2012). Irregular breathing in mice following genetic ablation of V2a neurons. J Neurosci 32: 7895–7906.
15. Okada Y, T Shimazaki, G Sobue and H Okano. (2004). Retinoic-acid-concentration-dependent acquisition of neural cell identity during *in vitro* differentiation of mouse embryonic stem cells. Dev Biol 275:124–142.
16. Ericson J, S Morton, A Kawakami, H Roelink and TM Jessell. (1996). Two critical periods of sonic hedgehog signaling required for the specification of motor neuron identity. Cell 87:661–673.
17. Ericson J, P Rashbass, A Schedl, S Brenner-Morton, A Kawakami, V Van Heyningen, TM Jessell and J Briscoe. (1997). Pax6 controls progenitor cell identity and neuronal fate in response to graded shh signaling. Cell 90:169–180.
18. Ericson J, J Briscoe, P Rashbass, V Van Heyningen and TM Jessell. (1997). Graded sonic hedgehog signaling and the specification of cell fate in the ventral neural tube. Cold Spring Harb Symp Quant Biol 62:451–466.
19. Sharma K, HZ Sheng, K Lettieri, H Li, A Karavanov, S Potter, H Westphal and SL Pfaff. (1998). Lim homeodomain factors lhx3 and lhx4 assign subtype identities for motor neurons. Cell 95:817–828.
20. Briscoe J, A Pierani, TM Jessell and J Ericson. (2000). A homeodomain protein code specifies progenitor cell identity and neuronal fate in the ventral neural tube. Cell 101:435–445.
21. Jessell TM. (2000). Neuronal specification in the spinal cord: inductive signals and transcriptional codes. Nat Rev Genet 1:20–29.
22. Pierani A, L Moran-Rivard, MJ Sunshine, DR Littman, M Goulding and TM Jessell. (2001). Control of interneuron fate in the developing spinal cord by the progenitor homeodomain protein dbx1. Neuron 29:367–384.
23. Thaler JP, SK Lee, LW Jurata, GN Gill and SL Pfaff. (2002). Lim factor lhx3 contributes to the specification of motor neuron and interneuron identity through cell-type-specific protein-protein interactions. Cell 110:237–249.
24. Li S, K Misra, MP Matise and M Xiang. (2005). Foxn4 acts synergistically with mash1 to specify subtype identity of v2 interneurons in the spinal cord. Proc Natl Acad Sci U S A 102:10688–10693.
25. Del Barrio MG, R Taveira-Marques, Y Muroyama, D-I Yuk, S Li, M Wines-Samuelson, J Shen, HK Smith, M Xiang, D Rowitch and WD Richardson. (2007). A regulatory network involving foxn4, mash1 and delta-like 4/notch1 generates V2a and V2b spinal interneurons from a common progenitor pool. Development 134:3427–3436.
26. Zhong G, S Droho, SA Crone, S Dietz, AC Kwan, WW Webb, K Sharma and RM Harris-Warrick. (2010). Electrophysiological characterization of V2a interneurons and their locomotor-related activity in the neonatal mouse spinal cord. J Neurosci 30:170–182.
27. Zhou Y, M Yamamoto and JD Engel. (2000). Gata2 is required for the generation of V2 interneurons. Development 127:3829–3838.
28. Karunaratne A, M Hargrave, A Poh and T Yamada. (2002). Gata proteins identify a novel ventral interneuron subclass in the developing chick spinal cord. Dev Biol 249:30–43.
29. Smith E, M Hargrave, T Yamada, CG Begley and MH Little. (2002). Coexpression of scl and gata3 in the V2 interneurons of the developing mouse spinal cord. Dev Dyn 224:231–237.
30. Kiehn O. (2006). Locomotor circuits in the mammalian spinal cord. Annu Rev Neurosci 29:279–306.
31. Al-Mosawie A, JM Wilson and RM Brownstone. (2007). Heterogeneity of V2-derived interneurons in the adult mouse spinal cord. Eur J Neurosci 26:3003–3015.
32. Lundfald L, CE Restrepo, SJB Butt, C-Y Peng, S Droho, T Endo, HU Zeilhofer, K Sharma and O Kiehn. (2007). Phenotype of V2-derived interneurons and their relationship to the axon guidance molecule epha4 in the developing mouse spinal cord. Eur J Neurosci 26:2989–3002.
33. Li S, K Misra and M Xiang. (2010). A cre transgenic line for studying V2 neuronal lineages and functions in the spinal cord. Genesis 48:667–672.
34. Panayi H, E Panayiotou, M Orford, N Genethliou, R Mean, G Lapathitis, S Li, M Xiang, N Kessaris, WD Richardson and S Malas. (2010). Sox1 is required for the specification of a novel p2-derived interneuron subtype in the mouse ventral spinal cord. J Neurosci 30:12274–12280.
35. Gingras M, V Gagnon, S Minotti, HD Durham and F Berthod. (2007). Optimized protocols for isolation of primary motor neurons, astrocytes and microglia from embryonic mouse spinal cord. J Neurosci Methods 163:111–118.
36. Peljto M, JS Dasen, EO Mazzoni, TM Jessell and H Wichterle. (2010). Functional diversity of ESC-derived

motor neuron subtypes revealed through intraspinal transplantation. Cell Stem Cell 7:355–366.
37. Rutherford AD, N Dhomen, HK Smith and JC Sowden. (2004). Delayed expression of the crx gene and photoreceptor development in the chx10-deficient retina. Invest Ophthalmol Vis Sci 45:375–384.
38. Vugler A, J Lawrence, J Walsh, A Carr, C Gias, MA Semo, A Ahmado, L Da Cruz, P Andrews and P Coffey. (2007). Embryonic stem cells and retinal repair. Mech Dev 124: 807–829.
39. Schmittgen TD and KJ Livak. (2008). Analyzing real-time pcr data by the comparative c(t) method. Nat Protoc 3: 1101–1108.
40. Briscoe J and BG Novitch. (2008). Regulatory pathways linking progenitor patterning, cell fates and neurogenesis in the ventral neural tube. Philos Trans R Soc Lond B Biol Sci 363:57–70.
41. Dessaud E, AP Mcmahon and J Briscoe. (2008). Pattern formation in the vertebrate neural tube: a sonic hedgehog morphogen-regulated transcriptional network. Development 2503:2489–2503.
42. Wichterle H and M Peljto. (2008). Differentiation of mouse embryonic stem cells to spinal motor neurons. Curr Protoc Stem Cell Biol Chapter 1:Unit 1H.1.1-1H.1.9.
43. Wilson L, E Gale, D Chambers and M Maden. (2004). Retinoic acid and the control of dorsoventral patterning in the avian spinal cord. Dev Biol 269:433–446.
44. Skaggs K, DM Martin and BG Novitch. (2011). Regulation of spinal interneuron development by the olig-related protein bhlhb5 and notch signaling. Development 138:3199–3211.
45. Zhao X, J Liu and I Ahmad. (2002). Differentiation of embryonic stem cells into retinal neurons. Biochem Biophys Res Commun 297:177–184.
46. Grandbarbe L. (2003). Delta-notch signaling controls the generation of neurons/glia from neural stem cells in a stepwise process. Development 130:1391–1402.
47. Amoroso MW, GF Croft, DJ Williams, S O'keeffe, MA Carrasco, AR Davis, L Roybon, DH Oakley, T Maniatis, CE Henderson and H Wichterle. (2013). Accelerated high-yield generation of limb-innervating motor neurons from human stem cells. J Neurosci 33:574–586.
48. Li XJ, ZW Du, ED Zarnowska, M Pankratz, LO Hansen, RA Pearce and SC Zhang. (2005). Specification of motoneurons from human embryonic stem cells. Nat Biotechnol 23:215–221.

Address correspondence to:
Dr. Shelly E. Sakiyama-Elbert
Department of Biomedical Engineering
Washington University in St. Louis
1 Brookings Drive Box 1097
St. Louis, MO 63130

E-mail: sakiyama@wustl.edu

Received for publication December 19, 2013
Accepted after revision March 18, 2014
Prepublished on Liebert Instant Online March 20, 2014